Mechanics & Industry **21**, 613 (2020)

https://doi.org/10.1051/meca/2020079

Mechanics & Industry

Available online at:
www.mechanics-industry.org

Regular Article

# Effect of size and shape of copper alloys particles on the mechanical and tribological behavior of friction materials

Amira Sellami[1], Nesrine Hentati[1], Mohamed Kchaou[2,1], Mohammad Asaduzzaman Chowdhury[3], and Riadh Elleuch[1,*]

[1] Laboratory of Electro-Mechanical System (LASEM), National School of Engineers of Sfax (ENIS), University of Sfax, Sfax, Tunisia
[2] Industrial department, College of Engineering, University of Bisha, Bisha, Kingdom of Saudi Arabia
[3] Department of Mechanical Engineering, Dhaka University of Engineering and Technology, Gazipur, Bangladesh

Received: 21 April 2020 / Accepted: 29 September 2020

**Abstract.** Friction materials are composed of numerous ingredients which differ from nature and particles size. Each ingredient has its own impact on the mechanical and tribological behavior of the material. Brass ingredients have a great impact on the thermal gradient dissipation in the sliding contact between disc and brake pad material. In this research, the influence of different sizes and forms of brass ingredient was studied on the friction material behavior. The physical (density), mechanical (yield strength, young module) and thermal (thermal conductivity and specific heat) properties of the considered composites were characterized. Results proves that only physical and mechanical properties are sensitive to the changes in size and form of brass particles. The tribological behavior of the brake friction materials was also assessed using a pin-on-disc tribometer. The results show that bigger brass particles and their elongated shape allows it to be well embedded on the pad surface during braking application, and thus decreased wear rate . In contrast, the smaller particle decrease the friction stability and it rounded shape increase wear of the material since it tearing from the surface by abrasive wear.

**Keywords:** Copper alloys / friction materials / tribological behavior / mechanical properties

## 1 Introduction

Friction materials find their applications mainly in automotive disk brake pads and clutch facings. Facing materials slid against each other, thus they suffer wear: Dry sliding wear (where surfaces interact without lubrication) or lubricated sliding wear (where sliding surfaces are lubricated) [1]. Under some conditions, sliding wear can generate third body particles debris (hard particles from one or both sliding surfaces) which may be at the origin of abrasive wear: either sliding abrasive wear (in which the particles slide) or rolling abrasive wear (in which the particles roll over the surface) [1]. Whatever the type of wear, friction materials should satisfy a number of requirements such as good wear resistance, reliable shear strength at a wide range of temperatures and high normal pressures.

Brake pad materials are known as multi-component composites, that makes them very heterogeneous materials. This heterogeneous character comes directly from the heterogeneity related to their constituents in regards to number [2], morphology [3] and size [4]. Each ingredient has a well-defined role in contributing to the different mechanisms of friction and wear [5]. This makes the understanding and the studying of the tribological behavior of brake pad materials increasingly complicated [6]. Friction and wear behavior is affected not only by the nature of ingredients but also by the shape and the size of ingredients (called structural parameters) as well as by friction materials properties such as the physical, the chemical and the mechanical properties and also by braking conditions (pressure, braking speed, time, etc.) [7,8].

Under various braking situations, a friction film (a third body layer) is formed between the sliding surfaces and monitors the tribological performance. This film has two morphologies: loose granular film which fill the primary contact plateau generated by worn fibers and dense sheet film called secondary contact plateau, also called flat plates formed by the agglomeration of cut and crushed loose granular films [9,10].These flat plates intensify the third body abrasion, and lead to a friction coefficient stability [11]. The continuous wear agglomeration mechanisms and the increase of flat plates area on the friction surface are responsible of the specific wear rate decrease [12]. In fact, the formation of regular friction film contributes to lower friction coefficient and specific wear rate [13].

* e-mail: riadh.elleuch@gnet.tn

Among all these parameters that interact with each other, brake pad formulation seems to be the most influential on the friction materials performance. Indeed, some researcher found that the metal alloy elements induced by their fairly high thermal conductivity better dissipation of the heat induced by friction [14]. Previous work proved that, apart from worn fibers, brass particles consisted also on primary plateaus necessary to the formation and the expansion of the flat plates present at the sliding surface [15] which contributed to wear resistance and friction coefficient stability. It is therefore very important to understand the interrelationship between friction materials formulation (nature, size and shape of ingredients) friction and wear behavior to determine the durability of the material [16]. Several research, studied the effect of the size of particles on the tribological behavior of the brake pad materials [17,18]. In fact, Brass particle is necessary in the formulation of the friction materials since it dissipate the frictional heat created in the rubbed surface. Therefore the study of the effect of both size and shape of these particles on the tribological performance of the friction materials is become mandatory. Hence, it is of significance to seek a fundamental understanding of the relationship between structural state of third body using different brass particle morphology and the tribological properties, and that requires observing the friction surface. The challenge is to preserve the same manufacturing parameters in order to facilitate the identification and understanding of the impact of brass particle size and shape on the friction coefficient level and its stability as well as on the wear rate. Friction and wear mechanisms involved on worn surfaces of both materials were also studied using SEM (Scanning Electron Microscopic) observations and EDX (Energy Dispersive X-ray) analysis. The mechanical and thermal responses were also evaluated and correlated with tribological properties of studied materials.

## 2 Materials and methods

### 2.1 Materials

The investigated friction material samples are made by two commercial, organic matrix composite materials, noted “FM1” and “FM2”, both materials have the same composition (Tab. 1).

**Table 1.** Studied friction materials composition.

| Classification | Nature | Ingredient | Weight% |
|---|---|---|---|
| Binder | Organic | Phenolic resin | 14.2 |
| Filler | Mineral | Rockwool fibers | 14 |
| | | Glass fibers | 10 |
| Particles | Mineral | Aluminum oxide<br>Barite<br>Carbonate of calcium | 46.3 |
| | Organic | Carbonaceous particles | 13.8 |
| | Metallic | Brass | 1.7 |

The manufacturing process to produce the FM1 and the FM2 materials comprised four steps: mixing, cold performing, hot molding for 18 min at 150 °C and finally curing of the plates (with a surface of $400 \times 400$ mm$^2$ and a thickness of 16 mm) for 10 hours at 160 °C. The difference between these two materials is only in the size and the shape of the brass particles.

### 2.2 Copper alloy sizes and forms

SEM observations of brass particles used for the FM1 material were illustrated in Figure 1. These particles show a rough surface and have globally rounded and semi-angular shape with an average size of 80 μm (particles size varies between 40 and 200 μm).

SEM observations of brass particles used for the FM2 material were shown in Figure 2. As for the case of FM1 material, the surface of brass particles was rough. In addition to the semi-angular form, we found elongated particles with angular shape having very sharp edge angles. The average size of the brass particles is in order of 500 μm (particles size ranges from 150 to 1000 μm).

Microstructures of both materials were also observed by SEM (Figs. 3 and 4). For ingredients distribution on the surface, we could notice that there was no difference between the two materials. All the constituents were dispersed on the surface of both materials. Many carbonaceous particles (appearing in black) were identified. The barite, alumina and calcium carbonate, appearing in white, were distributed in the matrix in form of particles of sizes of a few tens of micrometers. Rockwool fibers (appearing in grey) were observed on the surface in a spherical shape with an average diameter of 200 μm. They were called “Rockwool shot” and had the same composition as the Rockwool fiber [5]. EDX maps of the main elements found on the surface of the pad is established to identify the brass component. Figure 3b is characterized with Cu and Zn elements which are more widely scattered over the surface, in contrast Figure 4b a well-defined areas is dominated by Zn and Cu elements which correspond to brass particle, appearing in white, which was larger (more than 600 μm) and more elongated in FM2 material.

### 2.3 Determination of the thermo-physical and the mechanical properties

The thermal (thermal conductivity and specific heat), physical (density) and mechanical (level of strength) properties of the considered materials FM1 and FM2 were characterized. Thermo-physical properties were determined using the Hot Disk Thermal Constants Analyser. For thermal conductivity measurements, they were conducted on two samples with a diameter of 50 mm and a thickness of 16 mm. The sensor was placed between the

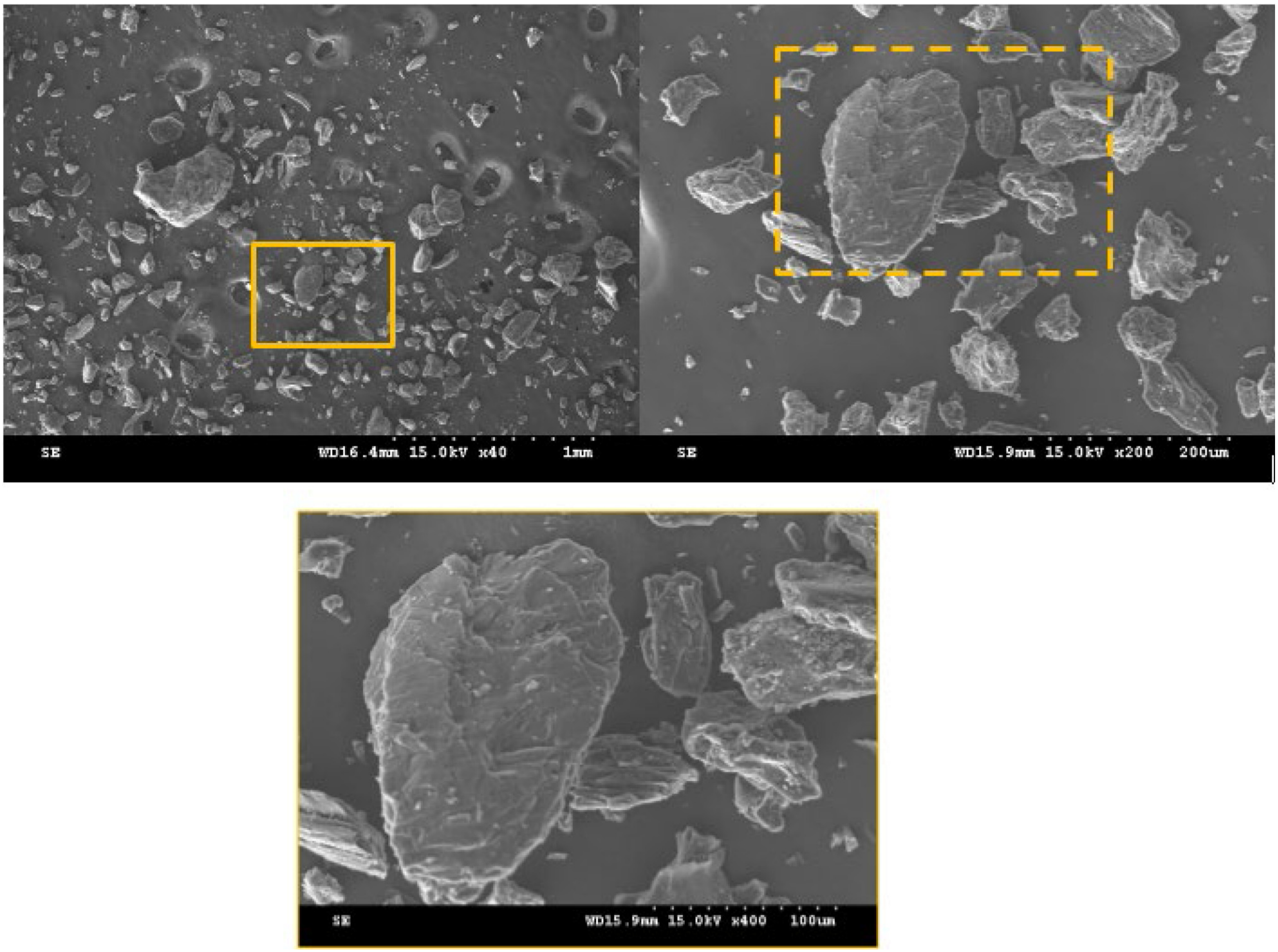


**Fig. 1.** SEM observations of brass particles of FM1.

two sample pieces. Thermogravimetric analysis allows the measurement of the loss of mass of a sample under the effect of thermal stress. It is carried out in order to assess the impact of temperature on the chemical stability of the friction material and to deduce the degradation temperatures. The test parameters used for our study are: a sample mass of 30 mg, a heating rate of 10 °C/min, a rise in ambient temperature up to 1200 °C and an oxidizing atmosphere (20% $O_2$ and 80% $N_2$). Concerning the specific heat, samples of 14 mm diameter and 4 mm thick were placed in an insulated gold container and carefully heated a few degrees with a well-defined heating effect, allowing very accurate calculation of specific heat. Mechanical tests were conducted on a universal testing machine (INSTRON1196). The diagram of the stress as a function of the strain is determined using the ASTM: D3039/D3039M − 08 standard test method. Tests were performed with a pre-load of 0.5 N and speed of 0.1 mm/min using four cylindrical specimens of diameter 14 mm and length 16 mm. Only normal direction was tested since it is the preferential direction relative to the real solicitation of the friction material [15]. In each experiment, five measurements are taken and the standard deviations were calculated.

## 2.4 Friction test

Friction-wear tests were conducted on a pin-disc type tribometer where the disc is mounted on the spindle axis (Fig. 5). A rotating collector mounted on the other end of the spindle axis induces its rotation via an electric motor. The application of the load is ensured by the action of a pneumatic loading. Two normal and tangential stress sensors are installed to record the applied load and the friction-induced tangential force.

The Tribometer ensured a plane-plane contact and measured the friction coefficient and the temperatures of samples in contact. The disc with lamellar graphite material (Tab. 2) had a radius of 35 mm. Friction cycles were programmed by controlling the contact time or the temperature thresholding. The samples temperature was monitored by two thermocouples; the first is set in

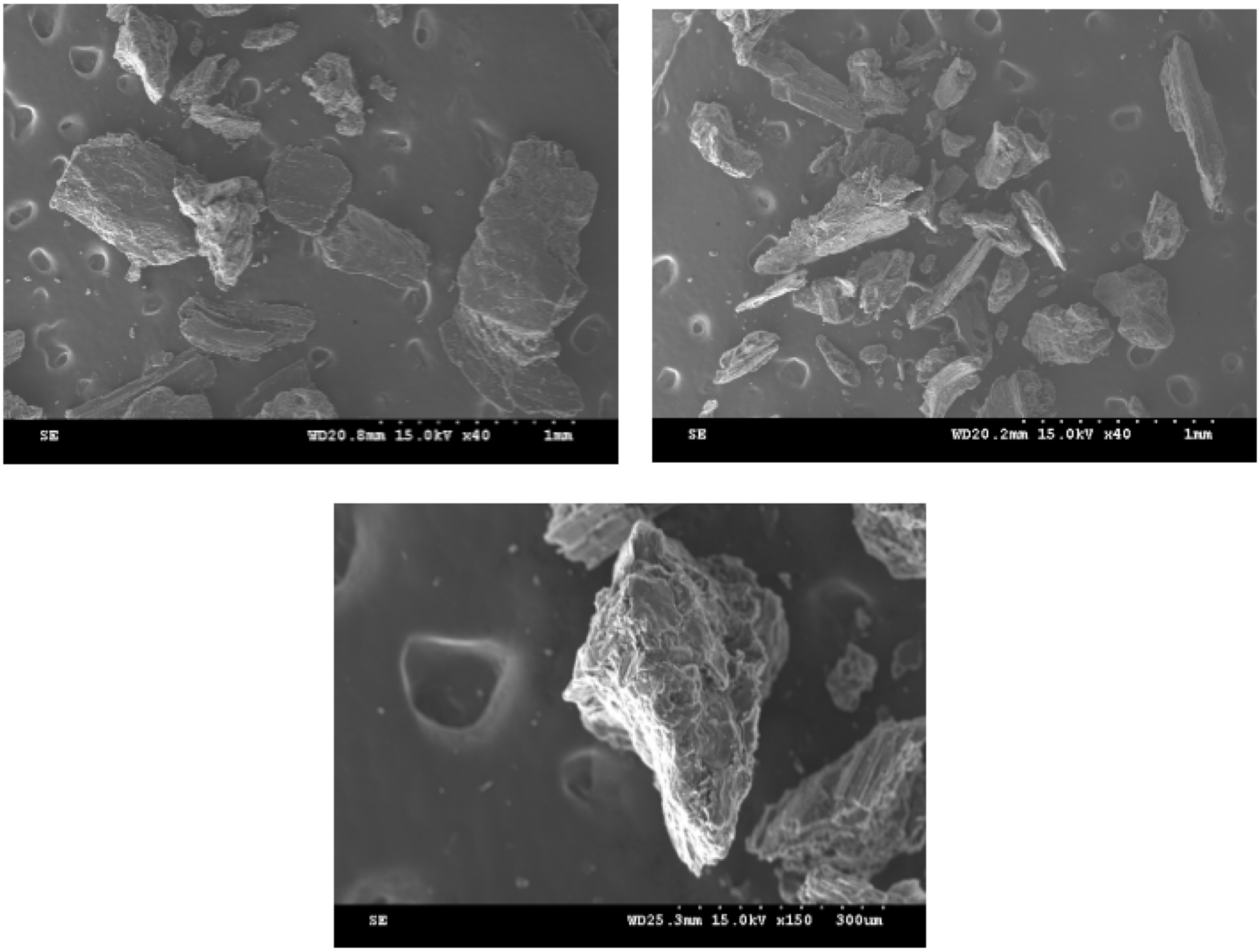


**Fig. 2.** SEM observations of brass particles of FM2.

**Table 2.** Chemical composition of lamellar graphite.

| Element | Fe | C | Si | Mn | Cu | Cr | S | Ni | P | Ti | Mo |
|---|---|---|---|---|---|---|---|---|---|---|---|
| W% | 92.41 | 3.41 | 2.23 | 0.68 | 0.62 | 0.37 | 0.13 | 0.06 | 0.04 | 0.02 | 0.02 |

the pin to 2 mm below the contact surface (denoted TP) and the second is set in the disc to 1 mm down the friction track (denoted TD).

Before conducting friction tests, samples were run in wear at 3 $ms^{-1}$ and 0.9 MPa for a maximum temperature of 90 °C to obtain at least 95% contact between the rubbing surfaces. Continuous wear test: characterized by high pressure (1.8 MPa) and sliding velocity (9 $ms^{-1}$). This test is controlled with disc temperature TD [50 °C–500 °C] until 5000 s of friction duration.

## 3 Results and discussion

### 3.1 Thermo-physical and mechanical properties

Thermo-physical as well as mechanical properties of both materials were summarized in Table 3. It is clear that the density decreased with the increase of the size of brass ingredients (FM2). However, thermal properties are not affected neither by brass particles size nor by their forms. Concerning mechanical response, it was noted that the friction material "FM2" which had the larger and the angular brass ingredient proved a higher rigidity since bigger metallic particles size were serving as rigid elements in the matrix.

### 3.2 Friction and temperature evolutions (tribological behavior)

According to several researchers, the friction coefficient, subjected to high-temperatures, decreased temporarily and this phenomenon was called "Fade" [19]. This latter was attributed to the thermal decomposition of ingredients following with the destruction of the third body present at the sliding contact which is responsible for the friction behavior of materials [20–22].

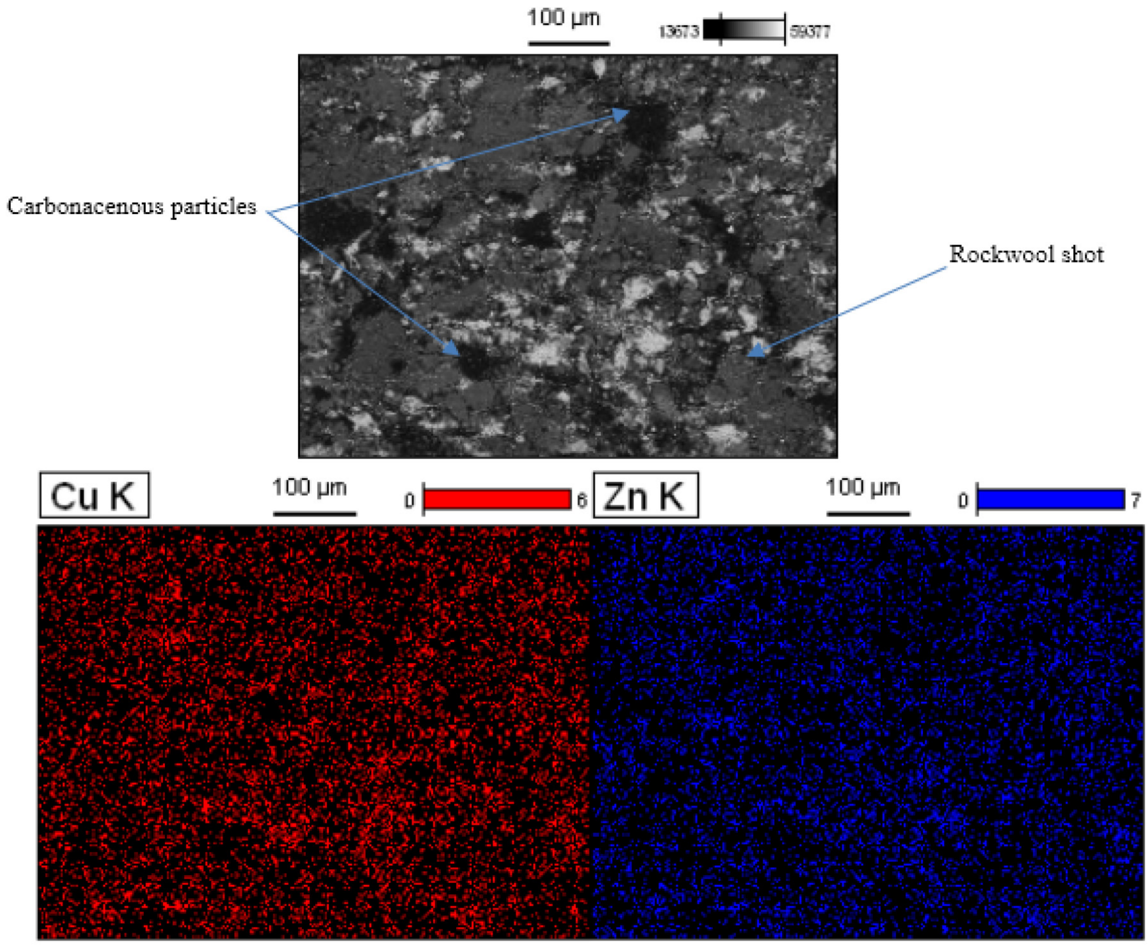


**Fig. 3.** (a) Morphology of the brake lining surface: FM1, (b) EDX mapping results.

**Table 3.** Thermo-physical and mechanical properties of investigated friction materials.

| | Friction material "FM1" | Friction material "FM2" |
|---|---|---|
| Specific heat($J \times kg \times K^{-1}$) | 673 (4.1) | 674 (3.1) |
| Thermal conductivity ($W \times m^{-1} \times K^{-1}$) | 1.04 (0.01) | 1.04 (0.015) |
| Density ($g/m^3$) | $2.3 \times 10^6$ | $1.8 \times 10^6$ |
| Max stress (MPa) | 98 (4) | 107 (2) |
| Max strain (%) | 6 (0.01) | 8 (0.02) |
| Yield modulus (GPa) | 1.6 (0.1) | 1.9 (0.2) |

*The value in parenthesis represents the standard deviation.

To investigate the fade phenomenon of samples, a continuous wear test was conducted until the disk temperature reached $500 \pm 10\,°C$. Figure 6 shows the evolution of the pin temperature (TP) as well as the friction coefficient ($\mu$) during the continuous wear test for the two materials FM1 and FM2.

From Figure 6, two phases could be distinguished: The first phase which extended up to 450 s (corresponding to a pin temperature rapid rise from 50 °C to 360 °C followed by the second phase which ended at 5000s where the pin temperature continued to increase slightly to reach 400 °C.

Figure 6 shows that during the first phase, the friction coefficient of each material increased up to an average of 0.45 for the first 100 s where the temperature had not yet exceeded 250 °C. Beyond this temperature, the friction coefficient dropped to reach about 0.16 at nearly 450 s for both materials. This result is consistent with the results in our previous work which showed that friction materials with brass fiber presented a pronounced drop in friction at 220–250 °C [14]. This behavior can be explained by the degradation of organic ingredients of the pad caused by the rise of the frictional heat generated at the friction interface.

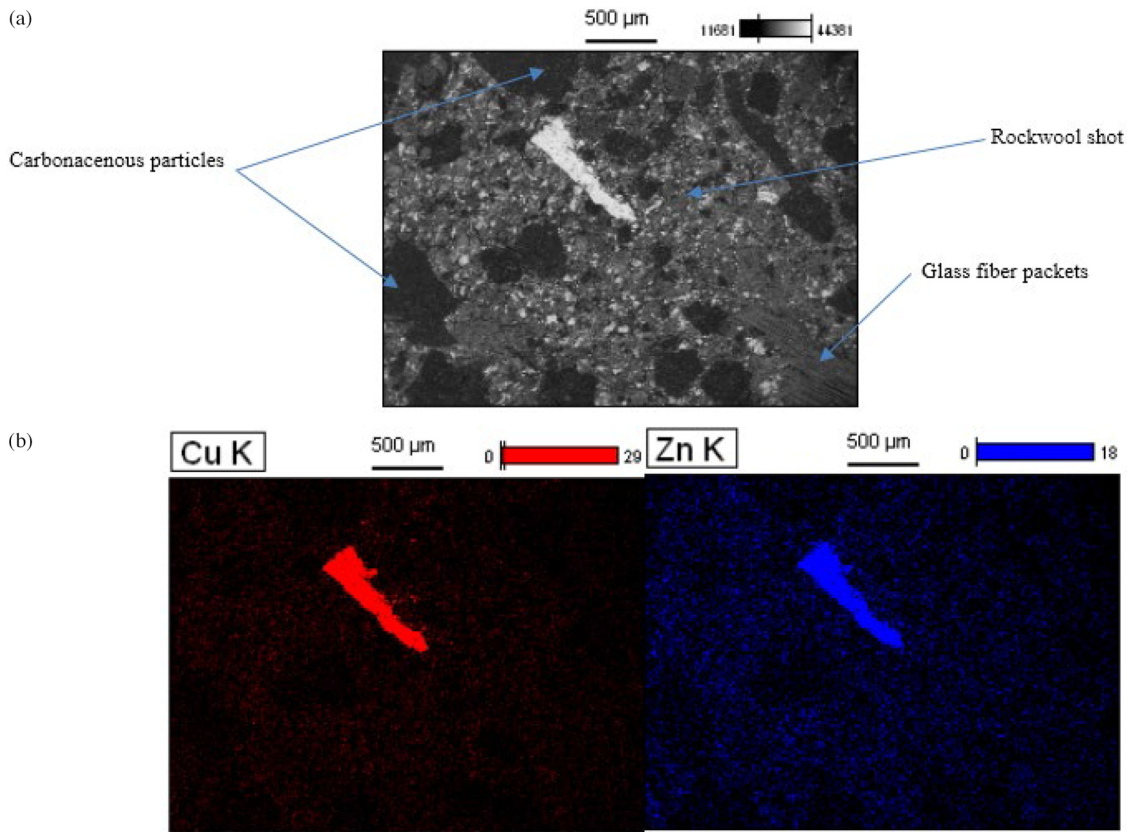


**Fig. 4.** (a) Morphology of the brake lining surface: FM2, (b) cartography results.

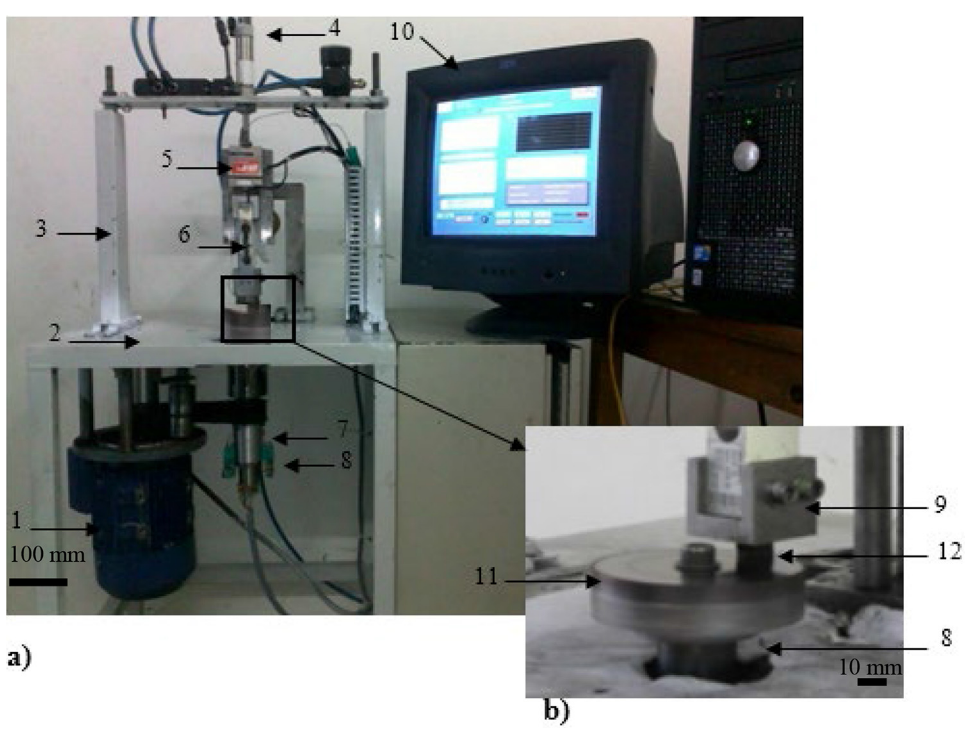


**Fig. 5.** (a) Pin-on-disc tribometer, (b) detail of the materials contact (1. Motor, 2. Table 3. Guidance, 4. Pneumatic loading, 5. Normal force sensor, 6. Tangential force sensor, 7. Spindle, 8. Rotating collector, 9. Slip ring, 10. Acquisition, 11. Disc, 12. Pin).

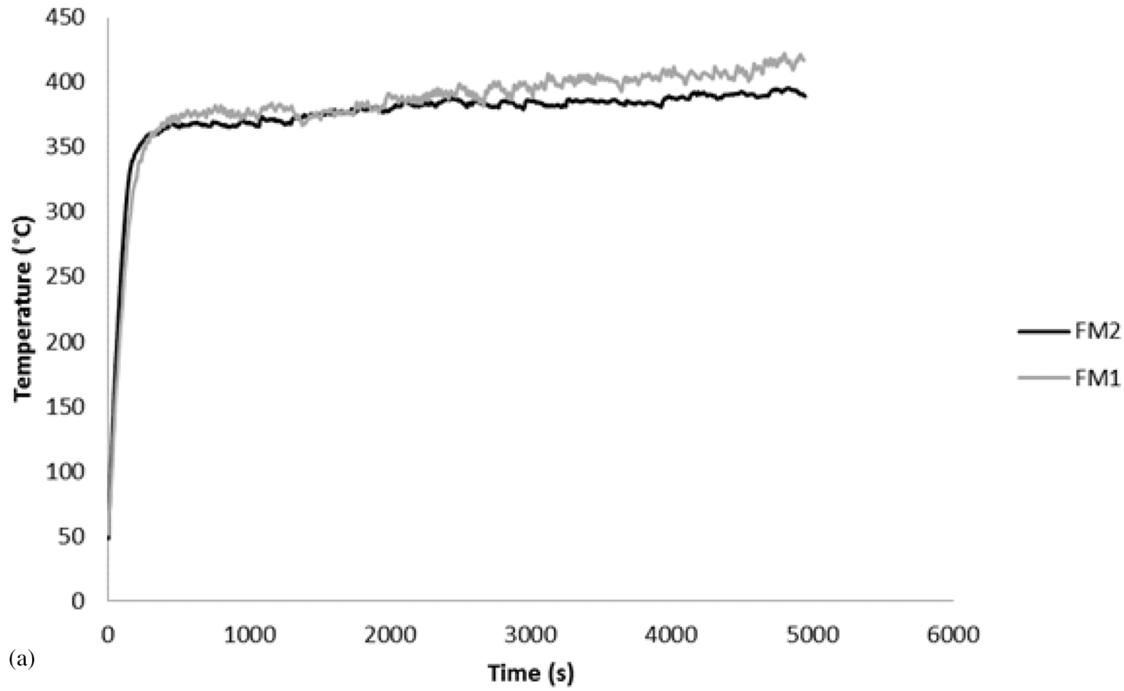


(a)

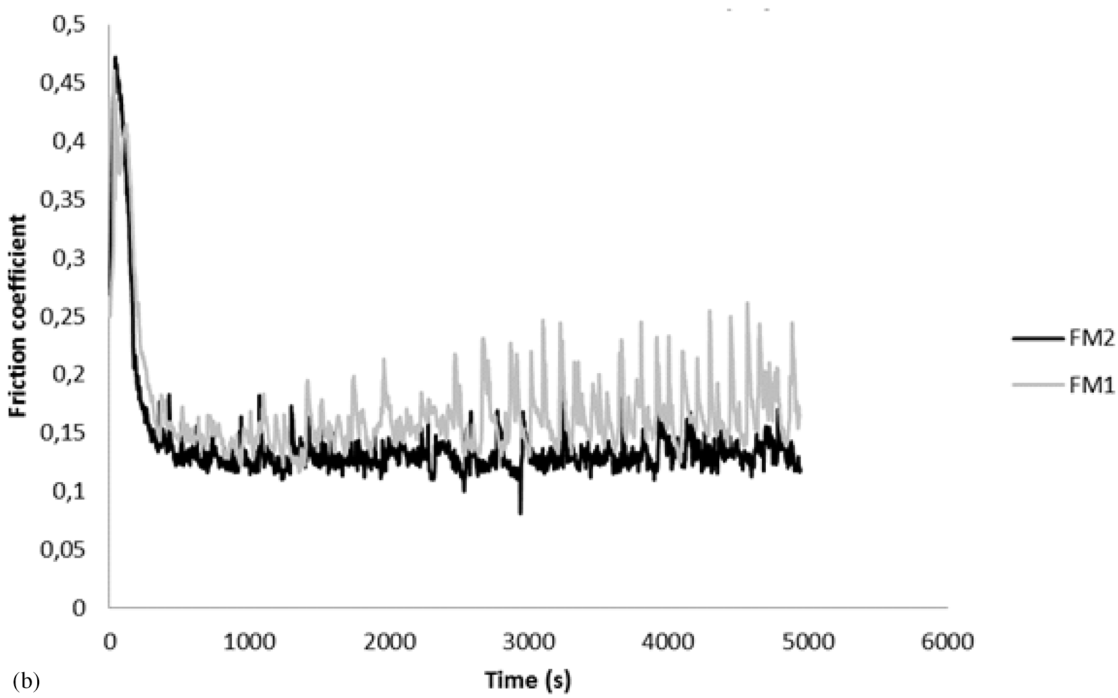


(b)

**Fig. 6.** (a) Temperature evolution and (b) friction coefficient evolution during the test.

The degradation of materials organic matrix friction starts from 230 °C and increases sharply between 270 and 400 °C [23]. Figure 7 confirms the first temperature degradation of the FM1 (about 250 °C) which is attributed to the degradation of the phenolic resin. The influence of the degradation of the resin results in instabilities of the changes in the coefficient of friction which attempt 0.45 for the first 100 s to decrease until an average of 0.16 at approximately 450s. Thus, the fade phenomena at elevated temperatures is attributed to the thermal decomposition of ingredients and followed by the subsequent destruction of contact areas at the sliding interface.

For the second phase, the friction coefficient values of both materials remained around 0.16. We could also note that during this phase, the friction coefficient of FM2 material (containing larger brass particles) was more stable with a less accentuated temperature than FM1 material.

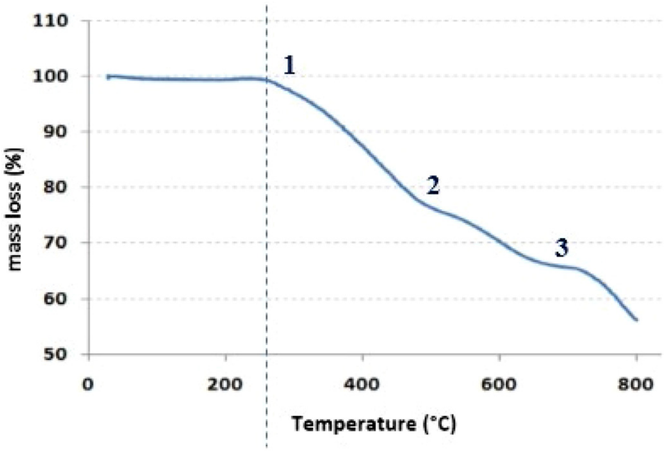


**Fig. 7.** Thermogravimetric analysis of the FM1. (1) 250 °C: 1st threshold degradation (degradation of the resin); (2, 3) 475 °C and 640 °C : Degradation thresholds for other constituents.

### 3.3 Contact surface topography

The worn surfaces of materials FM1 and FM2 were examined by SEM observations using back-scattered electrons mode and X-EDS analysis after the friction test in order to identify the friction mechanisms caused by friction in the brake lining pad/cast iron disc contact and to identify the chemical composition of selected area or point.

Both materials presented common findings. Rockwool shots were visible on the rubbed surfaces. They served as support for the compacted third body (flat plates) constituting thus primary plateau as well as carbonaceous particles as it was shown in the work of Erikson et al. [24]. The EDX analyses of the flat plate (Fig. 8b point 3 and Fig. 8b point 2) showed the presence of iron from the disc rubbed against the tested friction materials. Other elements such as silicon, aluminum, calcium and magnesium came from the mineral ingredients; calcium could also come from calcium carbonate. There was also barium from barite. The large amount of oxygen could come from the different materials ingredients, or metal oxides, especially iron oxide formed during the friction test. Glass fibers were also visible on the surface of materials FM1 and FM2. They were dispersed on the surface (Fig. 8a).

Concerning difference between the worn surfaces of both materials, it lied in brass particles contribution in friction and in flat plate's size. Indeed, worn surface of material FM1 (Fig. 8a) appeared less covered with compacted third body letting appear more particles, particularly brass particles which appears light gray (Fig. 8b point 2). In fact, the third body, which formed by the adhesion and compaction of wear particles is not well dispersed in the rubbed surface since the small size of the wear debris which is easily ejected out of the contact. Taking into account its rounded and semi-angular shape, brass particles are easier removed from the contact. Previous research proves that the bass element constitute a primary plates necessary to the formation and the expansion of the third body [4]. The brass particle is broken firstly and spread out (Fig. 8a), and then those fine particles squeezed out either flow out of the surface as wear debris or transfer to the inside of the contact, leading to form a brass pit (Fig. 8b). The third body particles are prone to fill in the fine brass pit, which becomes the nuclear area of the new third body formation but since their small size the third body is not well covering the rubbed surface. EDX results show that, as the test progresses, it can be seen that brass particles always exists in the fronts of third body formation. Therefore, since these particles are small size, the third body is not well compacted in the rubbed surface which explain the fluctuation of the friction coefficient.

Figures 9a and 10a shows numerous flat plates extended with millimeter size, covering the majority of the FM2 material surface, which may explain its more stable friction coefficient as has been shown in the work of Blau [25]. Also, brass particles were much less present on the rubbed surface of this material. EDX analysis (Fig. 9b, points 2–4) show that these light gray particles were covered with compacted third body. Indeed, the rubbed area is rich in Cu and Zn elements for the benefit of other elements. These other elements are due to the presence on the surface of particles of third body thus indicating the presence of brass particle richly covered with compacted third body. The EDX results of flat plates (Fig. 10b, points 3 and 4), show that brass particles appear mostly covered with compacted third body. They form primary plates that serve as support for the formation of plates of third body. In fact, angular particles entrapped more the third body layer to form more developed flat plates. Several researchers confirm that embedding is a function of particles size and shape and that embedding increases with elongated particles [26–28].

In this study, this behavior is also validated in the case of brass taking into account its shape and size. It is obvious from the SEM observations and the EDX analysis that when the brass particles were bigger with elongated and angular shape (FM2 material case), they remained embedded in the friction material surface forming thus primary plateaus. So, the third body agglomerated and compacted around them, enlarging the effective area of the contact plateaus and thus improved friction stability, while when they were smaller and rounded they were easily pulled out of the FM1 material surface. Some particles left definitively the contact to form wear debris and others recirculated in the contact to form third body in powder form. Obviously, these results clearly explain the better dissipation of the heat generated by the FM2 as long as it contains after friction a greater quantity of brass which has remained anchored to the matrix in the form of primary plates. In contrast to the FM1, the abduction of brass is reflected by a more accentuated temperature than that of FM2

Schematic drawings of the two different sliding interfaces caused by different brass sizes and shapes were given in Figure 11. They show that the primary contact plateaus of linings FM1 are composed of compacted wear debris containing small brass particles. On the other hand, large and elongated brass particles serve as primary contact plateaus and the compacted wear debris exist as secondary plateaus in the case of lining FM2. This observation suggested that the friction film provided effective contact plateaus and the oscillation of the friction coefficient was linked to the three-body abrasion of the

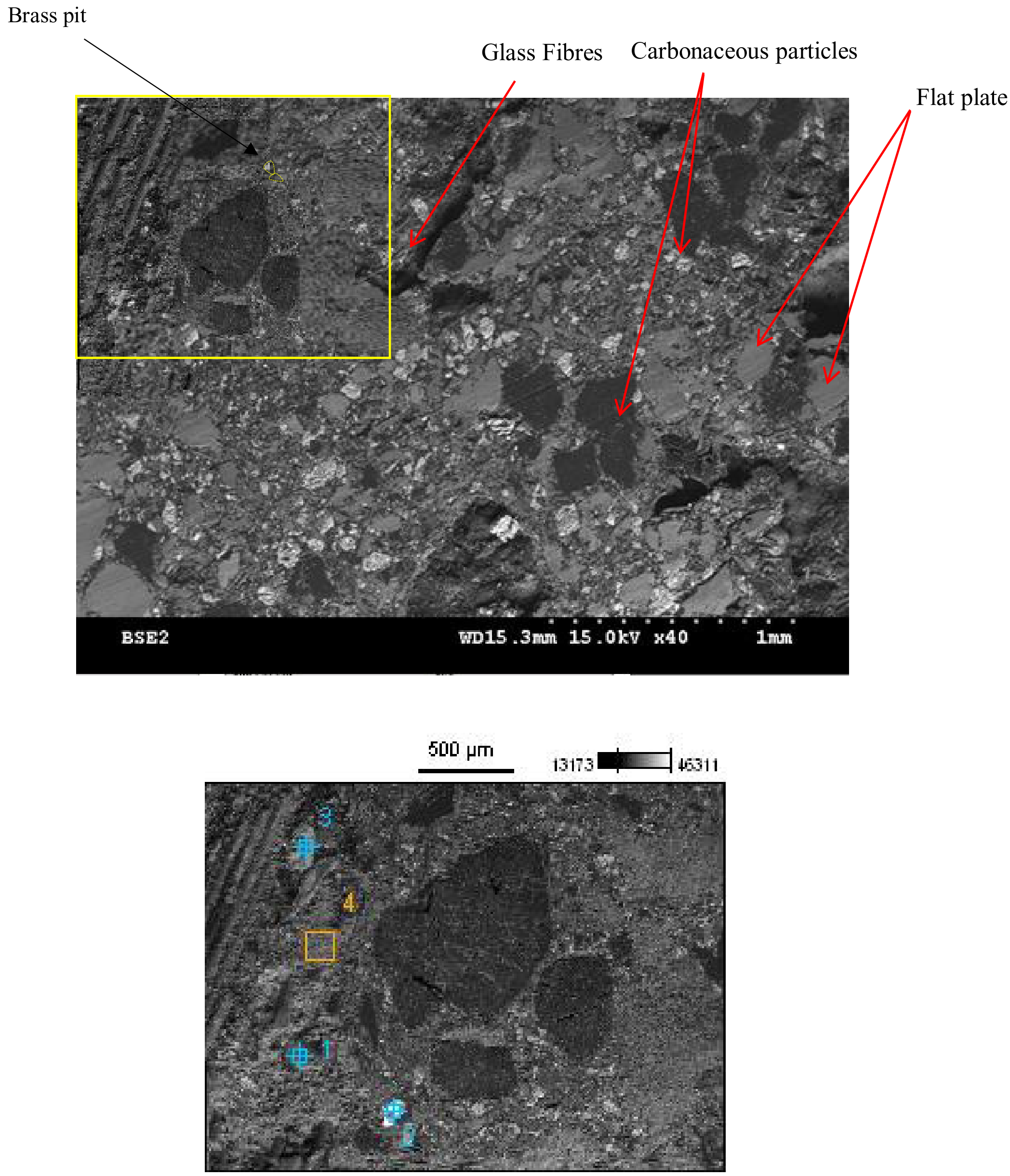


a)

b)

| | C | O | Mg | Al | Si | S | K | Ca | Fe | Cu | Zn | Br | Ba |
|---|---|---|---|---|---|---|---|---|---|---|---|---|---|
| *1* | 10.81 | 20.85 | | 0.83 | 4.59 | 1.53 | 0.24 | 3.42 | 34.96 | 8.11 | 5.35 | | 9.31 |
| *2* | 7.77 | 5.45 | | | 1.33 | | | 0.41 | 4.28 | 50.01 | 28.74 | 2.02 | |
| *3* | 6.30 | 10.20 | 0.13 | 1.06 | 4.46 | 1.13 | | 3.11 | 5.74 | 33.21 | 26.21 | | 7.45 |
| *4* | 11.84 | 21.03 | | 0.77 | 5.01 | 1.29 | | 3.23 | 35.35 | 8.26 | 4.46 | | 8.76 |

c)

**Fig. 8.** (a,b) Topography of the rubbed surface of FM1, (c) EDS results.

small brass particles at the sliding interface since the rolling action of the small particles destructed the friction film and transient contacts that increased the friction force oscillation. On the other hand, the worn surface of the lining FM2 was covered with a smooth friction film because the large brass particles were held tight in the brake lining.

## 3.4 Wear resistance

To characterize the wear behavior of the friction material, the mass loss was measured. As shown in Figure 12, FM2 material had lower wear rate which was attributed to its higher rigidity, as it was exhibited in Zhenga et al. study [12]. Indeed, they proves that the wear rate is directly

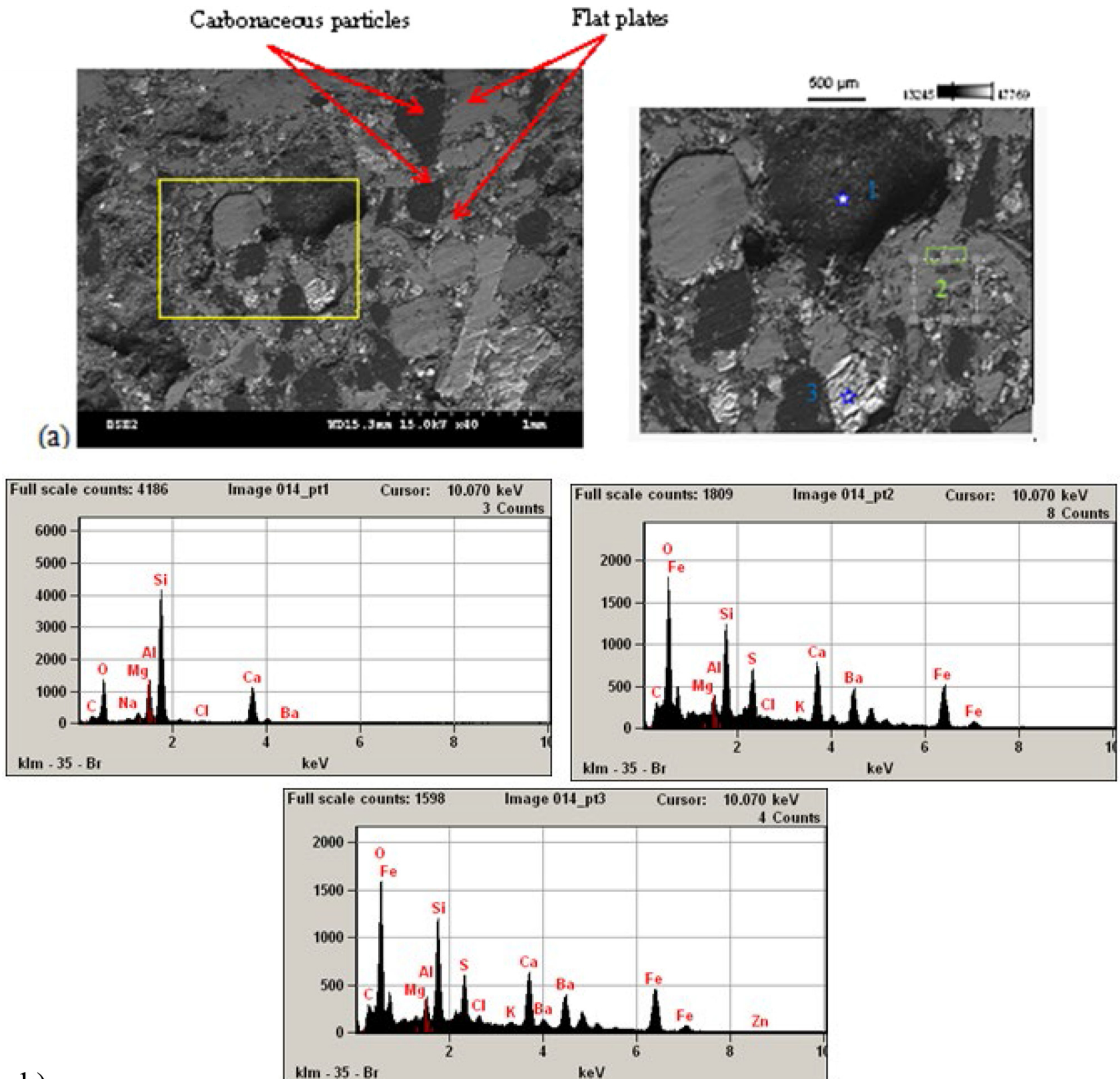


**Fig. 9.** (a) Topography of the rubbed surface of FM2, (b) EDS results.

proportional to the applied load and inversely proportional to the hardness of the material. Reduced specific wear rate was observed when brass particle size increases, most likely because of the evolution of the surface topography during sliding.

The good wear resistance of FM2 material could be also explained, according to other research work [29] to its bigger brass particles and to the elongated shape of these particles which allowed it to be well embedded on the pad surface during braking application, and thus deceased wear rate. It was reported also that wear resistance is greater with angular particles (FM2 material case) than rounded ones [30]. In fact, the rounded shape of brass particles enhances its rapid detachment from the matrix generating more wear debris, in other hand angular particles, as its previously shown, remains in the contact and forms a support for the formation and the expansion of the third body [17].

## 4 Conclusion

Mechanical and thermal properties as well as friction and wear behavior of two commercial friction materials which differ in brass particles form and size were studied.

The main conclusions are drawn as follow:

- Use of bigger and elongated brass particles affect mechanical properties (rigidity) in a beneficial way, but doesn't change thermal properties such as thermal conductivity and specific heat.

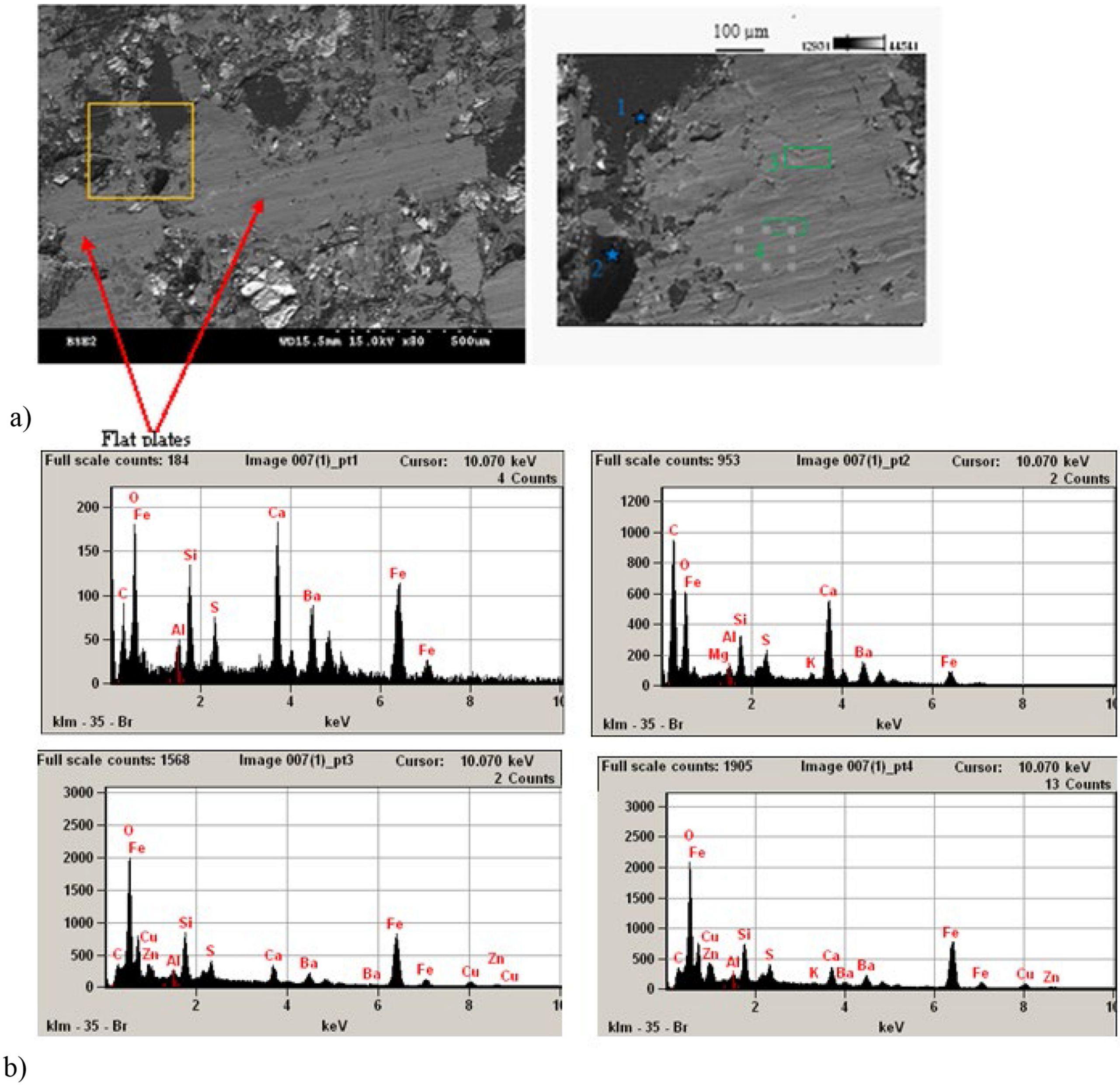


**Fig. 10.** (a) SEM of flat plates of FM2, (b) EDS results.

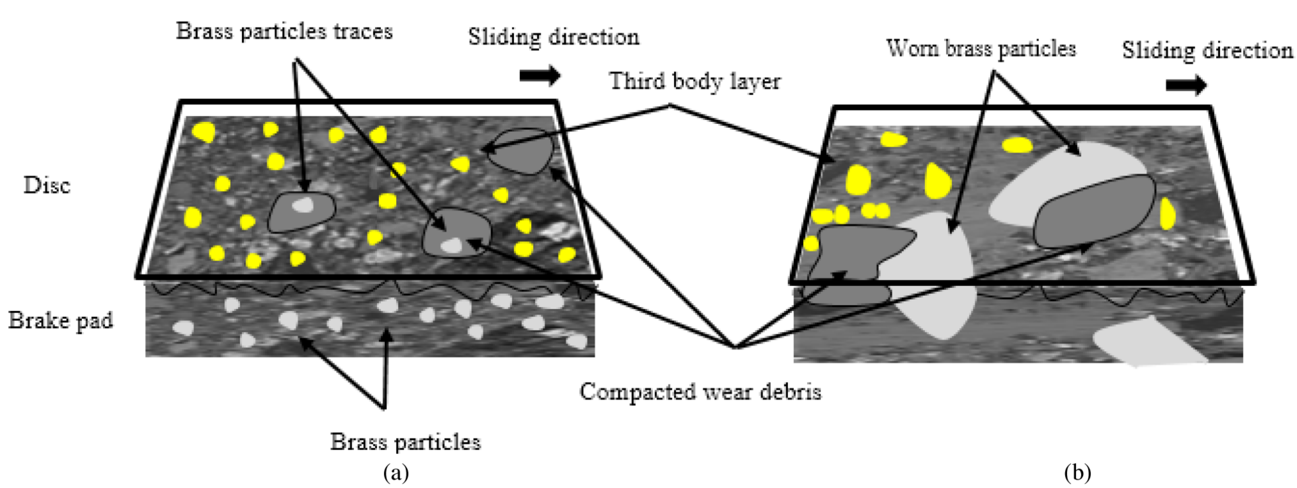


**Fig. 11.** Schematic representation of rubbed surface caused by different brass sizes and shapes: (a) FM1 and (b) FM2.

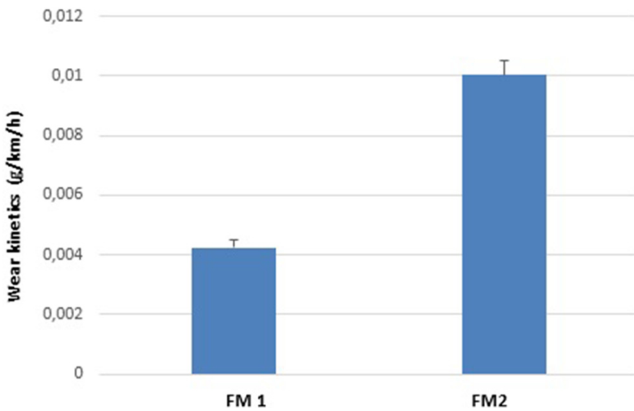


**Fig. 12.** Wear rate of materials FM1 and FM2.

- Inclusion of bigger and angular brass particles in friction material formulation enhanced friction coefficient stability.
- The shape of the particle highly affects its movement mode and thus changes the friction and wear.
- Big and angular brass particles are well embedded in pad surface and play so a favorable role of obstacles, leading to larger load-bearing flat plates. So the third body layer are compacted to form large and developed flat plates which sired quickly stabilization of the effective contact area This explains the good friction and wear behavior of friction material containing larger and angular brass particles.
- Fine particle sizes of brass particles causes the change in the morphology of third body. Specifically, the rounded and small size particles are rolled and mixed faster and easier with other wear debris to be ejected out of contact inducing a high surface roughness which is the main cause for unstable friction coefficient. Therefore a small-sized particle can decrease the friction stability and it rounded shape increase wear of the material.

The authors would like to thank the Tunisian Ministry of Higher Education and Scientific Research for their continuous support of research at the Laboratory of Electro-Mechanical Systems of Sfax. Special thanks are also due to STUGA Frem Society (Tunisia) for providing us with the brake lining samples.

## References


[1] I. Hutchings, P. Shipway, Sliding wear, Tribology (Second Edition)-Friction and wear of engineering materials, 107–164, (2017)

[2] M. Kchaou, A. Sellami, R. Kus, J. Fajoui, R. Elleuch, F. Jaquemin, Tribological performance characterization of brake friction materials: What test? What coefficient of friction?, Proceedings of the Institution of Mechanical Engineers, Part J: Journal of Engineering Tribology **233**, (2019)

[3] A. Sellami, M. Kchaou, R. Elleuch, A-L. Cristol, Y. Desplanques, Study of the interaction between microstructure, mechanical and tribo-performance of a commercial brake lining material, Materials and Design **59**, 84–93 (2014)

[4] M. Kumar, J. Bijwe, Optimized selection of metallic fillers for best combination of performance properties of friction materials: A comprehensive study, Wear **303**, 569–583 (2013)

[5] N. Hentati, M. Kchaou, A. Cristol, D. Najjar, R. Elleuch, Impact of post-curing duration on mechanical, thermal and tribological behavior of an organic friction material, Materials and Design **63**, 699–709 (2014)

[6] Y. Desplanques, O. Roussette, G. Degallaix, R. Copin, Y. Berthier, Analysis of tribological behavior of pad-disc contact in railway braking Part1. Laboratory test development, compromises between actual and simulated tribological triplets, Wear **262**, 582–591 (2007)

[7] R.H. Shen, L. He, Friction material and technology of its products. Beijing, China: Peking University Press, 2010

[8] J. Bao, Y. Yin, Y. Lu, Y.D. Hu, A cusp catastrophe model for the friction catastrophe of mine brake material in continuous repeated brakings. Proc IMechE, Part J: J Engineering Tribology **227**, 1150–1156 (2013)

[9] J.-J. Lee, J.-A. Lee, S. Kwon, J.-J. Kim, Effect of different reinforcement materials on the formation of secondary plateaus and friction properties in friction materials for automobiles, Triboogy International **120**, 70–79 (2018)

[10] X. Xiao, Y. Yin, J. Bao, L. Lu, X. Feng, Review on the friction and wear of brake materials, Advances in Mechanical Engineering **8**, 1–10 (2016)

[11] R.K. Uyyuru, M.K. Surappa, S. Brusethaug, Effect of reinforcement volume fraction and size distribution on the tribological behavior of Al-composite/brake pad tribo-couple, Wear **260**, 1248–1255 (2006)

[12] P. Zhanga, L. Zhanga, D. Weib, P. Wub, J. Caob, C. Shijiab, X. Qua, K. Fua, Effect of graphite type on the contact plateaus and friction properties of copper-based friction material for high-speed railway train, Wear 432–433 (2019)

[13] T. Peng, Q. Yan, G. Li, X. Zhang, Z. Wen, X. Jin, The braking behaviors of Cu-based metallic brake pad for high-speed train under different initial braking speed, Tribology Letters **65**, 135 (2017)

[14] A. Sellami, M. Kchaou, R. Kus, J. Fajoui, R. Elleuch, F. Jaquemin, Impact of brass contents on thermal, friction and wear properties of brake linings composites, Mechanics & Industry **19**, 605 (2018)

[15] M. Baklouti, A.L. Cristol, R. Elleuch, Y. Desplanques, Brass in brake linings: Key considerations for its replacement, Proceedings of the Institution of Mechanical Engineers Part J Journal of Engineering Tribology 208–210 (1994–1996)

[16] M. Kchaou, A. Sellami, A.R. Abu Bakar, A.R. Mat Lazim, R. Elleuch, S. Kumar, Brass fillers in friction materials composition: Tribological and brake squeal characterization for suitable effect evaluation, Steel and Composite Structures **19**, 939–952 (2015)

[17] M. Kumar, J. Bijwe, Non-asbestos organic (NAO) friction composites: Role of copper; its shape and amount, Wear **270**, 269–280 (2011)

[18] Y. Ha Chang, B. Soo Joo, S. Mok Lee, H. Jang, Size effect of tire rubber particles on tribological properties of brake friction materials, Wear **406–407**, 230 (2018)

[19] A. Ramadan, M.I. Khashaba, W.Y. Ali, Fade and temperature rise of automotive friction materials, Journal of the Egyptian Society of Tribology **8**, 53–66 (2011)

[20] B.K. Satapathy, J. Bijwe, Fade and Recovery Behavior of Non-Asbestos Organic (NAO) Composite Friction Materials based on Combinations of Rock Fibers and Organic Fibers, Journal of Reinforced Plastics and Composites **24**, 563–577 (2005)

[21] T.R. Jaafar, A.M. Zaharudin, A. Pahmi, R. Kasiran, E. Abu Othman, Effect of carbon in brake friction materials on friction characteristics, Journal of Engineering Science **14**, 47–59 (2018)

[22] M.K. Abdul Hamida, G.W. Stachowiak, S. Syahrullaila, The effect of external grit particle size on friction coefficients and grit embedment of brake friction material, Procedia Engineering **68**, 7–11 (2013)

[23] R.J. Talib, A. Muchtar, C.H. Azhar, Microstructural characteristics on the surface and subsurface of semi metallic automotive friction materials during braking process, Journal of Materials Processing Technology **140**, 694–709 (2003)

[24] M. Eriksson, F. Bergman, S. Jacobson, On the nature of tribological contact in automotive brakes, Wear **252**, 26–36 (2002)

[25] P.J. Blau, Microstructure and detachment mechanism of friction layers on the surface of brake shoes, Journal of Materials Engineering Performance **12**, 56–60 (2003)

[26] J. Day, X. Huang, N.L. Richards, Examination of a grit-blasting process for thermal spraying using statistical methods, Journal of Thermal Spray Technology **14**, 471–479 (2005)

[27] H. Getu, J.K. Spelt, M. Papini, Conditions leading to the embedding of angular and spherical particles during the solid particle erosion of polymers, Wear **292-293**, 159–168(2012)

[28] I. Hutchings, Ph. Shipway, Wear by hard particles, Tribology (Second Edition) Friction and Wear of Engineering Materials, 165–123 (2017)

[29] Ch. Jubsilp, J. Singto, W. Yamo, S. Rimdusit, Effect of graphite particle size on tribological and mechanical properties of polybenzoxazine composites, Chemical Engineering Transactions **57**, 1351–1356 (2017)

[30] I. Hutchings, P. Shipway, Wear by hard particles, Tribology (Second Edition)-Friction and wear of engineering materials, 165–236 (2017)

**Cite this article as**: A. Sellami, N. Hentati, M. Kchaou, M.A. Chowdhury, R. Elleuch, Effect of size and shape of copper alloys particles on the mechanical and tribological behavior of friction materials, Mechanics & Industry **21**, 613 (2020)